

Energetics and Mass Distribution of Fission Fragments in Triton- and Proton-Accompanied Fission of Cf^{252}

ERAN NARDI AND YAACOV GAZIT

Israel Atomic Energy Commission, Soreq Research Center, Yavne, Israel and Weizmann Institute of Science, Rehovot, Israel

AND

SEYMOUR KATCOFF†

Weizmann Institute of Science, Rehovot, Israel

(Received 17 December 1968)

The kinetic energies of the fission fragments and of the light particle emitted in triton- and proton-accompanied fission of Cf^{252} were measured in a four-parameter correlation experiment. Assuming that the average total kinetic energy of the fragments in long-range alpha fission (LRA fission) is 172.9 MeV, this value in triton-accompanied fission was found to be 173.5 ± 0.3 , while in proton-accompanied fission the value of 173.6 ± 0.5 was obtained. The mass distribution in triton-accompanied fission was found to be very similar to that in LRA fission, while this distribution for proton-accompanied fission is somewhat different from that in both binary and LRA fission. In addition, the degree of correlation between the average total fission-fragment energy and the particle energy was measured.

I. INTRODUCTION

IT has been demonstrated that quantitative information on the scission configuration of a fissioning nucleus can be obtained from the study of the long-range alpha (LRA) fission process.¹⁻³ By comparing the experimentally determined results of the LRA fission process to the results of trajectory calculations, the initial conditions at scission can be obtained within the framework of a given model for the scission configuration.

In addition to α particles, it has been established that other light nuclei, i.e., H^1 , H^2 , H^3 , He^6 , He^8 and Li , Be , B , and C isotopes are emitted in the fission process.⁴⁻⁷ However, the emission probabilities of these particles, which will be referred to in the following as light particles, are substantially lower than that of the α particle.^{4,5} For this reason the experimental properties of the light-particle fission process have been studied in much less detail than those of LRA fission.

The published experimental data concerning light-particle fission deal with the energy spectra of the various light particles emitted in the fission of Cf^{252} (Ref. 4, 5) and U^{236} * (Ref. 6) and with the angular distribution of these particles with respect to the direc-

tion of the fission fragments.⁷ However, in these experiments the energies of both fission fragments were not recorded simultaneously with the energy of the light particle. In LRA fission on the other hand, the fission-fragment energies were recorded in coincidence with the α particles and the experiments were performed as a function of the angle between the fission fragments and α -particle directions.^{8,9}

Raisbeck and Thomas⁷ used a three-point charge model in order to perform trajectory calculations of the different particles emitted in the fission of Cf^{252} . These authors found that reasonable agreement between the calculated and experimental spectra of the light particles could be obtained by assuming that the particles are released when the fission fragments are at a distance of 21.5×10^{-13} cm from each other. These calculations were carried out without reference to the energies of the fission fragments. Trajectory calculations were also carried out by Nardi, Boneh, and Fraenkel¹⁰; these authors obtained that the distance of the fission fragments at the time of particle emission is somewhat larger than in the calculations of Raisbeck and Thomas.

In this paper, we report the results of measurements of the properties of the fission fragments in fission accompanied by H^1 and H^3 . In Sec. II, we describe the experimental apparatus and procedure. In Sec. III, the experimental results are given. In Sec. IV, the results are discussed.

II. EXPERIMENTAL METHOD

Two fission-fragment detectors and two particle-telescope systems were placed inside a vacuum chamber

* Present address: Brookhaven National Laboratory, Upton, N.Y. 11973.

¹ B. T. Geilikman and G. I. Khlebnikov, *At. Energ. (USSR)* **18**, 218 (1963) [English transl.: *Soviet J. At. Energy* **18**, 274 (1965)].

² I. Halpern, CERN Report No. CERN-6812, 1963 (unpublished); *Physics and Chemistry of Fission* (International Atomic Energy Agency, Vienna, 1965), Vol. II, p. 369.

³ Y. Boneh, Z. Fraenkel, and I. Nebenzahl, *Phys. Rev.* **156**, 1305 (1967).

⁴ S. W. Cospers, J. Cerny, and R. C. Gatti, *Phys. Rev.* **154**, 1193 (1967).

⁵ S. L. Whetstone, Jr., and T. D. Thomas, *Phys. Rev.* **154**, 1174 (1967).

⁶ M. Dakowski, J. Chwaszczyńska, T. Krogulski, E. Piasecki, and M. Sowinski, *Phys. Letters* **25B**, 213 (1967).

⁷ G. M. Raisbeck and T. D. Thomas, *Phys. Rev.* **172**, 1272 (1968).

⁸ Z. Fraenkel, *Phys. Rev.* **156**, 1283 (1967).

⁹ Y. Gazit, A. Katase, G. Ben-David, and R. Moreh (to be published).

¹⁰ E. Nardi, Y. Boneh, and Z. Fraenkel, in *Proceedings of the Second Symposium on the Physics and Chemistry of Fission* (International Atomic Energy Agency, Vienna, to be published).

in the center of which was the Cf^{252} source. A schematic representation of the experiment is presented in Fig. 1. The fission counters were 300- Ω surface-barrier detectors of 20 mm diam. They were placed opposite each other at 45° to the plane of the source. The distance of the counters from the source was equal to 21 mm. The two particle telescopes were placed opposite each other at both sides of the Cf^{252} source and at 90° to the fission detectors. Each particle-telescope system consisted of a 100- μ dE/dx detector and a 1500- μ solid-state counter. The angle subtended by each telescope with respect to the source was 33° . In order to prevent fission fragments and 6.1-MeV α particles, from the Cf^{252} α decay, from reaching the particle-telescope detectors, a 19-mg/cm² gold foil was placed between the Cf^{252} source and dE/dx counter. The source consisted of Cf^{252} on a 100- $\mu\text{g}/\text{cm}^2$ Ni backing. The strength of the source was about 10^5 f/min.

The experiment performed was a four-parameter-correlation experiment. The recorded events consisted of the two pulses from each of the fission counters and two pulses from the same telescope system. The block diagram of the experimental system is given in Fig. 2. The four-dimensional Nuclear Data Inc. analyzer was gated by a coincidence pulse between the ($F1 \cap F2$) pulse and a pulse from either one of the particle telescopes. A special routing pulse was fed into the analyzer in order to distinguish between the two particle-telescope systems. The experimental data were collected during a period of about 100 days. Because of the damage inflicted on the fission counters by the fission fragments, these counters were calibrated every 24 h. This was accomplished by recording about 20 000 correlated binary-fission events in each calibration run. During the course of the experiment the fission counters were replaced once.

III. RESULTS

The experimental data were recorded on a magnetic tape and were analyzed with the aid of a CDC 1604A computer. A total of 410 protons in coincidence with both fission fragments were recorded. The number of such events involving tritons was 2290. In addition, the LRA fission events were analyzed as were the binary-fission events in order to check the experimental system and in order to compare them with the new experimental results.

A. Identification and Kinetic Energy of Particles

The identification of the light particles was accomplished using the method of Goulding *et al.*¹¹ However, these authors identified the particles on line, while here the analysis was carried out after the data were collected.

¹¹ F. S. Goulding, D. A. Landis, J. Cerny, and R. H. Pehl, IEEE Trans. Nucl. Sci. NS-13, 514 (1966).

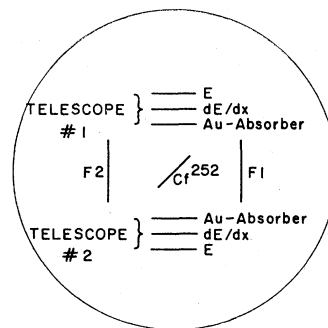


FIG. 1. Schematic representation of the experiment.

The method of Goulding *et al.* is based on empirical range-energy relation of light nuclei which is given by $R = aE^{1.73}$. Here R is the range of the particle, E is its kinetic energy, and a is a constant which depends on the mass and charge of the particle. If ΔE and E represent the pulse heights in the dE/dx and E detectors, respectively, and if T denotes the width in mg/cm² of the dE/dx counter, it follows:

$$T/a = (E + \Delta E)^{1.73} - E^{1.73}. \quad (1)$$

The particles were therefore identified on the basis of the T/a spectrum. In Fig. 3, for example, the T/a spectrum is plotted for the data obtained in particle telescope No. 2. In Fig. 3, it is seen that the deuteron peak is not well resolved from the larger triton peak. The broadening of these peaks due to the different distances penetrated by the particles through the dE/dx counter cannot account for the widths of the identification peaks. The reason for the poor resolution in the particle identification spectrum in the region of the hydrogen isotopes is therefore not understood.

Since a considerable number of counts under the deuteron peak are due to triton events, the results obtained here for the hydrogen isotopes were confined only to the properties of the protons and the tritons.

The kinetic energy spectra for the protons and tritons are shown in Fig. 4. The proton spectrum in Fig. 4(a) is plotted together with the results of Raisbeck and Thomas⁷ which were obtained at 90° to the direction of the fission fragments. Both spectra are in satisfactory agreement; however, the slope in the spectrum of Raisbeck and Thomas is somewhat larger than that obtained in our experiment. It should be added that neither spectrum agrees with the results of Cospers *et al.*⁴ who obtained a peak in the proton spectrum in the region of 8 MeV. The latter measurements, however, were not carried out in coincidence with the fission fragments and, as a result, an appreciable amount of background may have been present. This background was attributed mainly to the 6.1-MeV α particles from the decay of Cf^{252} .⁴

A possible source of proton background may be the (n, p) reactions resulting from the prompt fission

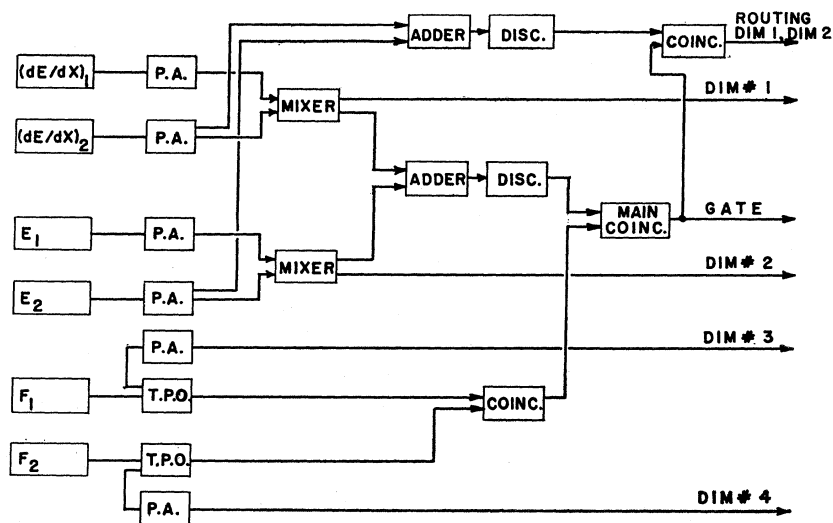


FIG. 2. Block diagram of experiment. P.A. stands for preamplifier and T.P.O. for "time pickoff unit."

neutrons which are in coincidence with the fission fragments. These secondary protons should be produced by the interaction of the neutrons with the particle telescopes. Hence, as pointed out by Raisbeck and Thomas,⁷ the strong correlations between the direction of the fission fragments and prompt neutrons should cause the secondary protons to be peaked at 0° and 180° with respect to the direction of the fragment. The experimental results of these authors show that the proton spectrum is peaked at 90° . However, the width of their angular distribution curve is much broader than that for the other light particles (with the possible exception of H^2), indicating that some (n, p) background may be present in the proton spectrum. Since our experiment was carried out in essentially the same manner as that of Raisbeck and Thomas, we conclude that our proton spectrum may include some contribution of neutron-induced secondary protons.

In the following, the properties of the fission fragments will be given for protons of energy greater than 6 MeV, for tritons of energy greater than 8 MeV, and for α particles of energy greater than 16.5 MeV. These energies are the cutoff energies of the light particles in our experiment.

B. Kinetic-Energy Spectra of the Fission Fragments

The energy calibration of the fission counters was carried out by assuming a linear dependence between fission-fragment energy and detector pulse height. This assumption was made since the dependence of the "pulse-height defect" on the mass and energy of the fission fragments is unknown for counters damaged by fission fragments.

The energy-versus-pulse-height calibration curve was obtained from the positions of the heavy and light fragment peaks of the binary-fission single-fragment kinetic energy spectrum. The energies of these peaks were taken from the "time-of-flight" values of Whet-

stone¹² and were corrected for prompt neutron emission from the fragments. The heavy and light peak energies thus obtained were 79.5 and 104.3 MeV, respectively. Following the method of Whetstone, the positions of the peaks were obtained by fitting the single-fragment kinetic energy spectrum to two Gaussian distributions.

The single-fragment kinetic energy spectra of proton-, triton-, and α -accompanied fission are plotted in Fig. 5. The results of triton- and α -accompanied fission are very similar. In proton-accompanied fission, however, the distance between the heavy and light fragment peaks is smaller than in the above two cases and the relative widths of the peaks are also different. The experimental data were fitted to the sum of two Gaussian distributions. The fits were carried out with both equal and statistical γ^{-1} weightings. The results are presented in Table I; the results for binary fission are also included in Table I.

The total-fragment kinetic energy spectra for proton-,

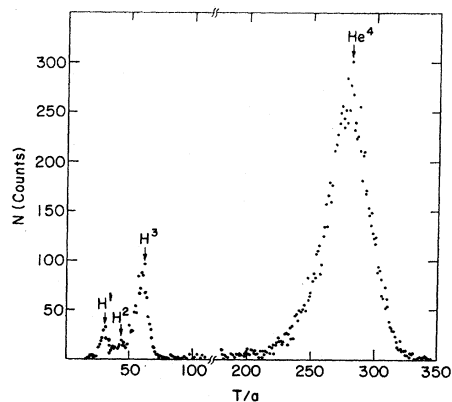


FIG. 3. The particle identification spectrum obtained in telescope No. 2. The abscissa is in units of $(\text{MeV})^{1.72}$.

¹² S. L. Whetstone, Jr., Phys. Rev. 131, 1232 (1963).

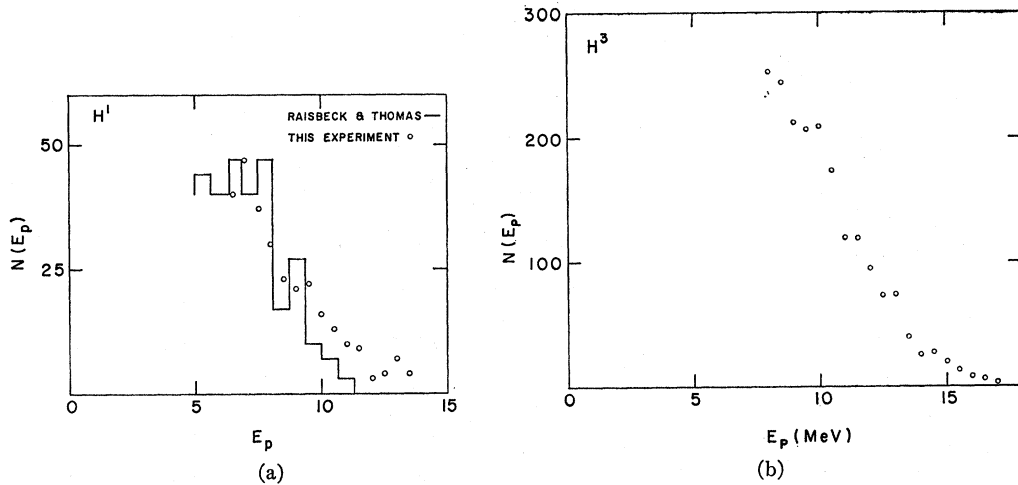


FIG. 4. The kinetic-energy (MeV) spectra of light particles. (a) Proton data together with the results of Raisbeck and Thomas (Ref. 7). (b) Triton spectrum.

triton-, and α -accompanied fission are observed in Fig. 6 to be very similar to each other. The Gaussian fitted values of these spectra are given in Table I. The mean total kinetic energy of the fission fragments (E_F)_{AV} was also calculated. The results are as follows: in proton fission 173.6 ± 0.5 MeV, in triton fission 172.7 ± 0.2 MeV, in α fission 171.5 MeV, and in binary fission 183.0 MeV.

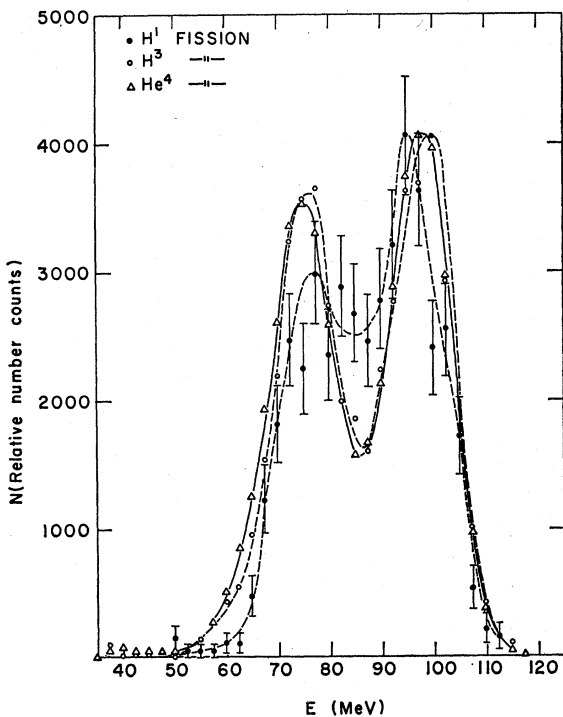


FIG. 5. The single-fragment-kinetic energy spectra in proton-, triton-, and α -accompanied fission. The error bars are for proton-accompanied fission.

C. Mass Distribution of the Fission Fragments

The mass distribution of the fission fragments were obtained from the energy ratios of the fission fragments. The effect of the light-particle recoil was also accounted for. We denote by M_H and M_L the heavy and light fragment masses, and by E_H and E_L the heavy and light kinetic energies of the fragments. The connection between mass ratio and energy ratio is given by

$$E_L/E_H = (M_H/M_L) [1 - (M_P E_P / M_H E_H) \cos \theta_L]^2. \quad (2)$$

The quantity within the bracket is due to the light-

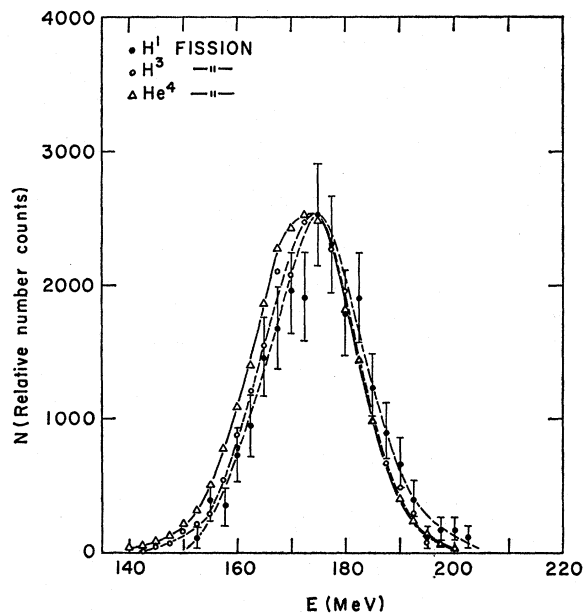


FIG. 6. The total fission-fragment kinetic-energy spectrum in proton-, triton-, and α -accompanied fission. The error bars are for proton-accompanied fission.

TABLE I. Mean values and standard deviations of distributions.

Parameter \ Fission mode	H ¹	H ³	He ⁴	Binary
Equal weighting				
\bar{E}_H	77.01±0.92	75.22±0.23	74.83±0.11	79.72±0.10
σ_{E_H}	6.99±0.92	6.60±0.23	7.09±0.12	8.29±0.11
\bar{E}_L	95.72±0.82	97.86±0.20	97.73±0.09	104.50±0.07
σ_{E_L}	6.88±0.68	6.01±0.20	5.81±0.09	6.52±0.07
\bar{E}_F	174.80±0.54	173.45±0.19	172.39±0.13	184.17±0.11
σ_{E_F}	9.49±0.54	9.06±0.19	9.30±0.13	10.39±0.11
\bar{M}_L	112.34±0.50	107.98±0.19	106.16±0.10	109.12±0.08
σ_{M_L}	7.28±0.54	6.82±0.19	7.00±0.10	7.80±0.08
\bar{M}_H	138.66±0.48	140.98±0.19	141.84±0.10	142.88±0.08
σ_{M_H}	7.00±0.51	6.84±0.19	7.00±0.10	7.80±0.08
γ^{-1} Weighting				
\bar{E}_H	76.40±0.86	75.82±0.32	74.85±0.18	79.50±0.18
σ_{E_H}	5.70±0.50	7.33±0.27	7.57±0.15	8.78±0.14
E_L	94.75±0.75	98.02±0.26	97.82±0.14	104.30±0.13
σ_{E_L}	6.98±0.51	5.76±0.19	5.69±0.10	6.40±0.10
\bar{E}_F	174.90±0.45	173.25±0.18	172.15±0.11	183.78±0.15
σ_{E_F}	9.36±0.34	9.06±0.14	9.38±0.08	10.43±0.12
\bar{M}_L	112.00±0.48	107.68±0.24	106.10±0.12	108.92±0.15
σ_{M_L}	7.16±0.42	6.96±0.20	7.14±0.12	7.96±0.13
\bar{M}_H	139.04±0.48	141.22±0.24	141.90±0.12	143.08±0.15
σ_{M_H}	7.12±0.40	6.98±0.20	7.14±0.12	7.96±0.10

particle recoil, while M_P and E_P denote the mass and kinetic energy of the light particle. Since θ_L , the angle between the light particle and the light fission fragment, was not measured in this experiment, the most probable value of θ_L was used in Eq. (2). For α particles, this was found experimentally to be 82° ,⁸ while for protons and tritons the predicted values of Nardi *et al.*¹⁰ were taken. These values are 84° for protons and 83° for tritons.

The effect of prompt neutron emission on the mass distribution curves was not accounted for, since no data on prompt neutron emission in proton- and triton-accompanied fission are available. For comparison, the mass distributions in LRA and binary fission were also calculated in this manner, although the average number of neutrons as a function of fragment mass are known.^{13,14} Therefore, Eq. (2) does not give accurately the preneutron emission mass distribution,

but the error involved in this procedure was found to be relatively small in binary fission.¹⁵

The mass distributions in proton-, triton-, and α -accompanied fission are given in Fig. 7(a), while the fitted values of the mass distributions are given in Table I. The triton- and α -accompanied mass distributions are observed to be very similar, the widths of the mass distributions are equal within the margin of error (see Table I). The peak value of the light fragments is about two mass units lower in α fission than in triton fission, while in the case of the heavy fragments, the α fission peak is about one mass higher than that in triton fission. The proton mass distribution is observed to differ substantially from the α and triton fission mass distributions. In Fig. 7(b), the proton mass distribution is plotted together with the binary mass distribution and the heavy and light peaks are both seen to be shifted in the direction of symmetric fission, in the case of the light fragments by three mass units and in

¹³ H. R. Bowman, J. C. D. Milton, S. G. Thompson, and W. J. Swiatecki, Phys. Rev. **129**, 2133 (1962).

¹⁴ E. Nardi and Z. Fraenkel, Phys. Rev. Letters **20**, 1248 (1968).

¹⁵ H. W. Schmitt, J. H. Neiler, and F. J. Walter, Phys. Rev. **141**, 1146 (1966).

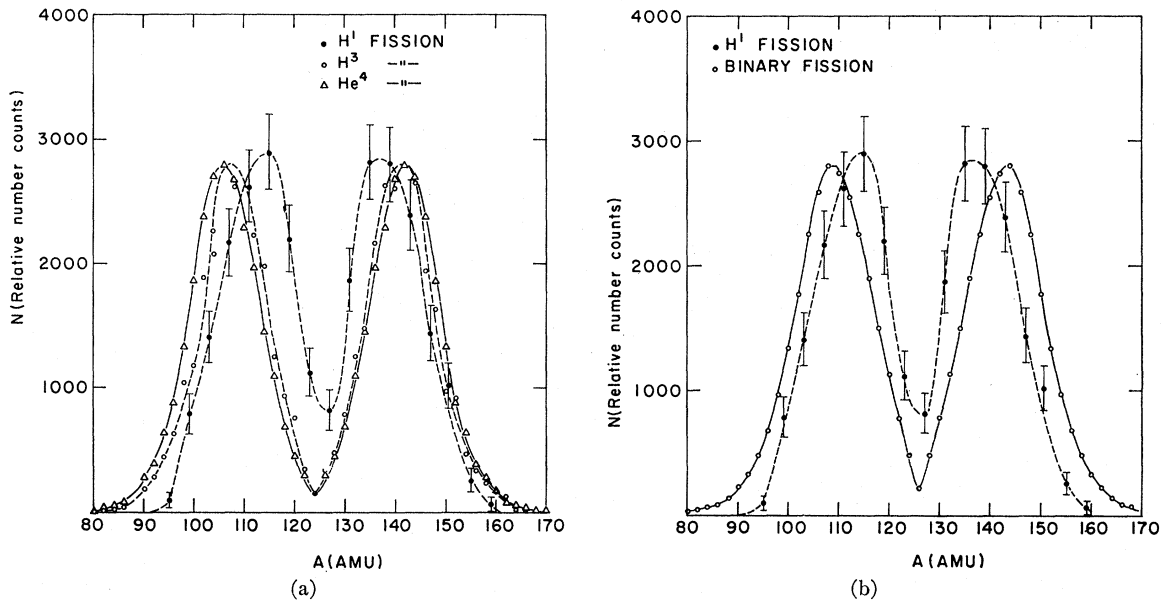


FIG. 7. The mass distributions obtained for (a) proton-, triton-, and α -accompanied fission, (b) proton-accompanied fission and binary fission. The error bars are for proton-accompanied fission.

the case of the heavy fragments by four masses. The proton-accompanied mass distribution was also obtained for protons of energy greater than 8 MeV. This also agreed within the statistical uncertainties with the results of Fig. 7(b).

The mean total kinetic energy \bar{E}_F of the fission fragments is plotted in Fig. 8 as a function of the mass of the heavy fission fragment A_H for particle-accompanied

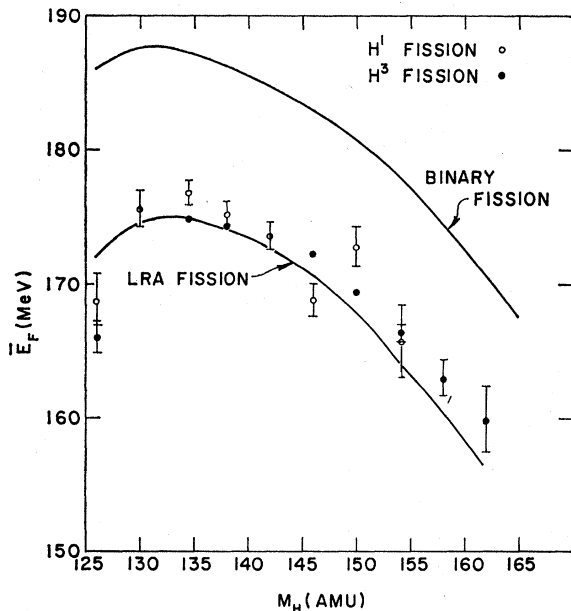


FIG. 8. The average total fission-fragment kinetic energy as a function of the mass of the heavy fragment in proton-, triton-, and α -accompanied fission and in binary fission.

fission and for binary fission. The variation of \bar{E}_F as a function of A_H is observed to be very similar for all the modes of fission shown in the figure.

D. Correlation between Total Fragment Kinetic Energy and Particle Energy

The average total kinetic energy of the fission fragments \bar{E}_F was studied as a function of the energy of light particle E_P . The results are given in Fig. 9. The solid lines in the figures are the results of a weighted least-square fit of the data. These results are as follows:

$$\Delta \bar{E}_F / \Delta E_P = -0.04 \pm 0.20, \quad \text{for protons,}$$

$$\Delta \bar{E}_F / \Delta E_P = -0.37 \pm 0.10, \quad \text{for tritons,}$$

$$\Delta \bar{E}_F / \Delta E_P = -0.41 \pm 0.05, \quad \text{for } \alpha\text{'s.}$$

Fraenkel⁸ obtained for α particles a value of -0.445 ; this result, however, was obtained for α particles between 10 and 19 MeV.

IV. DISCUSSION

The results of the experiment performed here show that the energetics and mass distribution in triton-accompanied fission closely resemble those properties in LRA and binary fission. These results, therefore, indicate that the scission properties of triton-accompanied fission should resemble those in binary and LRA fission.

It is of interest to compare the values of the average total kinetic energy of the three particles (i.e., fission fragments plus light particle) in LRA- and triton-accompanied fission. In calculating this quantity, it must be recalled that the fission fragments were

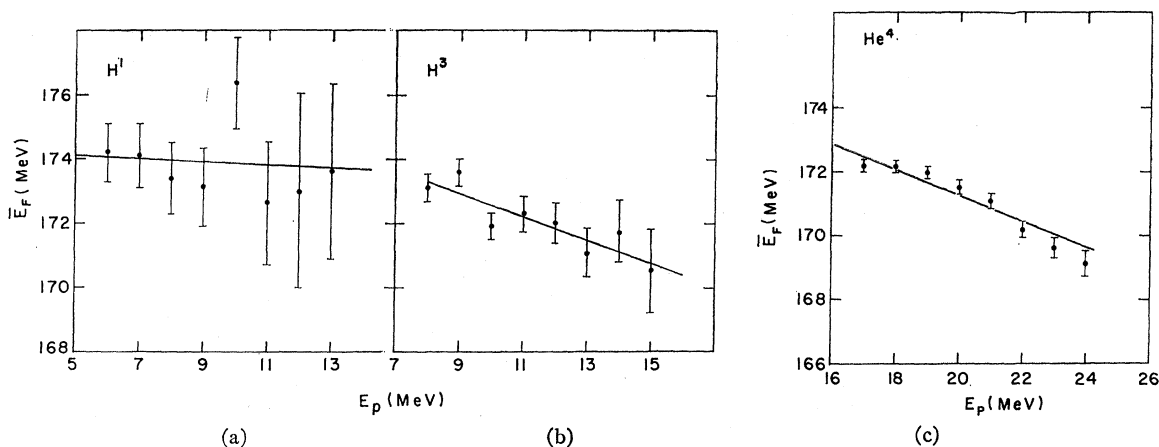


FIG. 9. The average total fission-fragment kinetic energy as a function of particle energy in (a) proton-accompanied fission, (b) triton-accompanied fission, (c) LRA fission.

measured for α particles and tritons of energies greater than 16.5 and 8.0 MeV, respectively. Due to the negative correlation between the average fragment kinetic energy and light-particle energy (see Fig. 9), the exclusion of the low-energy particles causes the measured value of the average fragment kinetic energy for *all* particles emitted to be lower than its real value. In order to correct for this effect, we assume that the slope of the \bar{E}_F -versus- E_p curve of Fig. 9 remains unchanged at particle energies below the cutoff values of the experiment. In addition, we assume that the light-particle spectra are of Gaussian shape extending to zero energy, and the peak and standard deviations of these spectra are those obtained by Cospers *et al.*⁴ The value of \bar{E}_F , the average fragments kinetic energy for *all* emitted α particles of all energies would then be 1.4 ± 0.15 MeV higher than the value obtained in this experiment; in triton-accompanied fission, \bar{E}_F for *all* tritons is 0.8 ± 0.2 MeV higher than our measured quantity. The corrected values of \bar{E}_F are, therefore, 172.9 ± 0.15 MeV in LRA fission and 173.5 ± 0.3 MeV in triton-accompanied fission.

The average *total* kinetic energy of the three-particle system \bar{E}_T , is assumed to be equal to the value of \bar{E}_F found above plus the most probable particle kinetic energy as determined by Cospers *et al.*⁴ The \bar{E}_T values are, therefore, as follows: in LRA fission 188.9 ± 0.3 MeV, and in triton-accompanied fission 181.5 ± 0.4 MeV. \bar{E}_T in LRA fission is, therefore, 7.4 ± 0.45 MeV higher than in triton-accompanied fission. If it were assumed as in the trajectory calculations of Raisbeck and Thomas⁷ that the initial conditions at scission are identical in LRA- and triton-accompanied (i.e., equality in the initial kinetic energies of the fission fragments and light particles and equal distance between fragments), then the difference in \bar{E}_T between LRA and triton fission would be well approximated by $3 \times 49 \times e^2/D$. Here D denotes the distance between the fragments. The value of D obtained on the basis of the

above experiment and from the energy difference obtained in this experiment is (28.5 ± 1.7) F. This value is substantially higher than that obtained by Raisbeck and Thomas.⁷

Since there is essentially no correlation between the proton kinetic energy and fragment kinetic energy, we obtain that \bar{E}_F for *all* emitted protons is equal to 173.6 ± 0.5 MeV, the experimental value obtained here. The results of Raisbeck and Thomas⁷ seem to indicate that the most probable kinetic energy of the protons is equal to 6 MeV. Based on this value (which is somewhat in doubt), we obtain that \bar{E}_T in proton fission is 179.6 ± 0.5 MeV. This value is lower than that in triton fission by 1.9 ± 0.7 MeV. The proximity in the values of \bar{E}_T perhaps indicates that the scission configurations in both processes do not differ by too much. Detailed trajectory calculations will, however, furnish more information on this point.

The degree of negative correlation between the average fragment kinetic energy and the energy of the light particle appears (Fig. 9) to be greater in triton- than in proton-accompanied fission. This quantity, as has been pointed out by Boneh, Fraenkel, and Nebenzahl⁸ is strongly dependent on the initial conditions at scission. However, assuming the initial conditions at scission to be similar, the degrees of correlation would be expected to be greater as the mass of the particle increases, since the lighter the particle the more rapidly will the particle leave the field of the fission fragments, and thus its influence on the motion of the fission fragments will be smaller than for a heavier particle.

The most striking feature of the experiment performed here is perhaps the result that the mass-distribution curve and single-fragment kinetic energy spectrum in proton-accompanied fission differ from these results obtained in the other modes of fission studied here. It was mentioned that background events due to the 6.1-MeV α particles of Cf^{252} probably do not appear in

the proton spectrum, while background due to prompt fission neutrons might very well be present in this spectrum. The latter type of background would, however, cause the mass-distribution curve to resemble that of binary fission. Hence, this type of background cannot account for the different behavior of the proton fission mass distribution.

The anomalous behavior of proton-accompanied fission has been previously pointed out by Raisbeck and Thomas⁷ in connection with the energy spectrum and angular distribution of these particles. The results of our experiment, therefore, indicate that the different behavior of proton-accompanied fission is also observed in connection with the properties of the fission frag-

ments. It should, however, be added that the behavior of the total fragment kinetic energy distribution and of the average fragment kinetic energy as a function of fragment mass are in proton fission similar to the other fission modes studied here. Proton-accompanied fission is perhaps at this stage the least understood mode of light-particle fission and further experimental work would be useful to the understanding of this process.

ACKNOWLEDGMENTS

The authors are very thankful to Professor Zeev Fraenkel for his very helpful advice and criticism. One of the authors (S.K.) is grateful to the Guggenheim Foundation for a grant.

Low-Yield Products from Fission of Th²³², U²³⁵, and U²³⁸ with 14.8-MeV Neutrons*

D. R. NETHAWAY, B. MENDOZA, AND T. E. VOSS

Lawrence Radiation Laboratory, University of California, Livermore, California 94550

(Received 12 August 1968; revised manuscript received 18 February 1969)

We have measured the fission yields of a number of products from 14.8-MeV neutron fission of Th²³², U²³⁵, and U²³⁸. The fission products chosen are all on the wings of the mass-yield curves and are formed in very low yield. They extend from Ni⁶⁶ to Zn⁷² and from Sm¹⁵³ to Er¹⁷². The amount formed of each product was determined by absolute β and γ counting techniques. The number of fissions in each target was calculated from the target mass, the fission cross section, and the neutron flux. The neutron flux was measured by means of the Y⁸⁹ ($n, 2n$) Y⁸⁸ reaction with Y₂O₃ monitor foils. The results show that, within experimental uncertainty, the wings of the mass-yield curves are consistent with Gaussian functions. These Gaussian curves allow interpolation and prediction of fission yields of unmeasured products. The widths of the mass-yield curves for U²³⁵ and U²³⁸ are almost the same, while that of Th²³² is significantly narrower. The centers of the Gaussian distributions are shifted to higher mass numbers than would be predicted from the average total neutron emission in fission. The effect of target impurities on the measured fission yields was shown to be generally small. An attempt was made to examine the effect of nuclear charge distribution on the mass yields. This effect, which would cause the observed fission yields to be less than the total mass yield, is probably significant only for the yields of masses 166 and 172. As a check on our experimental method we also remeasured the fission yields of three products near the peaks of the mass-yield curves. Our results are consistent with those reported before.

INTRODUCTION

THE mass-yield curves for the fission of Th²³², U²³⁵, and U²³⁸ induced by 14-MeV neutrons have been characterized fairly well in the areas of high fission yield. Much fewer experimental data have been reported for products formed in low yield. This has been due mainly to the relatively weak sources of 14-MeV neutrons that are available, compared, for example, to sources of thermal or reactor neutrons. The amount of experimental data obtained for 14-MeV neutron fission is still large compared to that obtained for fast neutron fission at other energies. The deuterium-tritium fusion reaction ($d+t \rightarrow n+\alpha$) provides a unique source of monoenergetic neutrons with energy about 14 MeV.

For U²³⁵ and U²³⁸ the data taken at 14 MeV indicate the usual double-humped asymmetric mass-yield distribution.¹⁻⁴ For 14-MeV neutron fission of Th²³² this asymmetric distribution is modified by a small central peak due to symmetric fission.⁵⁻⁸

Very few data exist for the products on the wings of the mass-yield curves. For Th²³² no yields have been reported below mass 83 or above mass 157. For U²³⁵

¹ S. Katcoff, *Nucleonics* **18**, 201 (1960).

² D. G. Vallis and A. O. Thomas, Atomic Weapons Research Establishment Report No. AWRE-O-58-61, 1962 (unpublished).

³ M. P. Menon and P. K. Kuroda, *J. Inorg. Nucl. Chem.* **26**, 401 (1964).

⁴ R. H. James, G. R. Martin, and D. J. Silvester, *Radiochimica Acta* **3**, 76 (1964).

⁵ K. M. Broom, *Phys. Rev.* **133**, B874 (1964).

⁶ S. J. Lyle, G. R. Martin, and J. E. Whitley, *Radiochimica Acta* **3**, 80 (1964).

⁷ R. Ganapathy and P. K. Kuroda, *J. Inorg. Nucl. Chem.* **28**, 2071 (1966).

⁸ T. Mo and M. N. Rao, *J. Inorg. Nucl. Chem.* **30**, 345 (1968).

* Work performed under the auspices of the U.S. Atomic Energy Commission.